

The Effect of a Low-Viscosity Swelling Liquid on the Tensile Strength of Rubber

K. A. GROSCH, *The Natural Rubber Producers' Research Association, Welwyn Garden City, Hertfordshire, England*

Synopsis

The paper examines the effect of swelling on a number of different gum rubbers and rubbers filled with different types and concentrations of black. The observed decrease in strength with decreasing rubber fraction V_r (increasing swelling ratio) is, in the case of gum rubbers, associated with a decrease in internal friction. The incorporation of a black filler is shown to increase strength by hydrodynamic stiffening and by an increase in internal friction of the rubber network, and a simple reduction scheme of the data shows a close analogy between the strength as a function of V_r and the dynamic modulus of a rubber solution as a function of concentration. The results lead to a failure criterion, which describes the energy density at break as a simple function of the hysteresis near break.

INTRODUCTION

Swelling decreases the strength of rubber in two ways. First, the swelling liquid subjects the network to a dilatational deformation. On this basis Taylor and Darin¹ predict that the breaking extension, measured on the swollen sample, should be proportional to $V_r^{1/3}$, where V_r is the rubber fraction in the swollen rubber. This, however, is obeyed only at low rubber fractions (high swelling ratios).² For lightly swollen rubbers a second effect, the diminution in molecular cohesion and its effect on strength, far outweighs the dilatational effect. Greensmith et al.² find that the elongation at break for lightly swollen rubbers decreases more rapidly than predicted by Taylor and Darin. Wildschut³ shows that the decrease in strength depends on the type of rubber, and Dogadkin et al.,⁴ by using swelling liquids of different physical and chemical properties, show that the change in strength with increasing swelling ratio depends also on the type of swelling liquid and a strong interaction exists between the types of rubber and liquid.

Information on the effect of internal friction on the strength of swollen rubbers is sparse. The effect of hysteresis on the strength of dry rubbers has been more thoroughly studied with rate and temperature as variables. From such investigations it is known that the strength of noncrystallizing gum rubbers is predominantly derived from the hysteresis in the rubber.^{5,6} Natural rubber exhibits low internal friction at low strains but becomes

highly hysteretical, when it crystallizes at high strains, and is then very strong.^{7,8} Above a critical extension rate and temperature crystallization cannot take place, and NR is then very weak.^{9,10}

Similarly, it is known that the hysteresis in a carbon-black-filled rubber increases with strain,¹¹⁻¹⁴ and the reinforcing action of carbon black has been associated with the increased hysteresis,¹⁵ which the black confers to the rubber at high strains, although the exact mechanism remains obscure. However, the recent work of Harwood et al.¹⁶ on stress softening has done much to elucidate the nature of hysteresis in black-filled rubbers.

The present investigation, in which swelling is a variable, was undertaken to examine quantitatively the effect of hysteresis on the strength of a wide range of rubbers, including noncrystallizing gum rubbers, crystallizing natural rubber, and a range of rubbers filled both with different types and different concentrations of black filler.

EXPERIMENTAL

Ring specimens, cut from a sheet by means of a rotary cutter, were weighed dry, immersed in the swelling liquid for various times, and then placed in sealed bottles for at least 24 hr. Since the equilibrium swelling ratio was reached after approximately 4 hr., this allowed sufficient time for the liquid to distribute itself uniformly throughout the sample. Bromobenzene was used as the swelling liquid for all experiments. This produced large swelling ratios rapidly without too great an evaporation rate during the extension measurements.

Before the start of the extension the rings were reweighed and then stretched to break on the Instron tester at a constant crosshead speed of 20 cm./sec. and a constant ambient temperature of 21°C. The rings were reweighed after the experiment. It was found that they had lost between 1 and 5% of the absorbed liquid, and the swelling ratios were calculated from the average weight before and after the experiment.

The internal diameter of the ring was 1.62 cm., but this increased to 1.7 times this value for a fully swollen gum rubber; hence the extension rate varied with the swelling ratio.

The complete stress-strain curve was recorded, and from this the energy density to break, the tensile strength, and the elongation to break were obtained.

The results are expressed in terms of the rubber fraction V_r , contained in unit volume of swollen compound. This is related to the swelling ratio V_s by

$$V_r = 1/V_s \quad (1)$$

The swelling ratio is calculated from

$$V_s = 1 + d_r/kd_e(M_s/M_0 - 1) \quad (2)$$

where k is the rubber fraction by weight in the *dry* compound, d_r and d_e are the rubber and liquid densities, and M_s and M_0 are the weights of the swollen and dry sample, respectively.

RESULTS AND DISCUSSION

Gum Rubbers

Elongation at Break. Figure 1 shows the elongation at break referred to the swollen length of the test piece as a function of $V_r^{1/3}$ for four gum rubbers of natural rubber (NR), styrene-butadiene rubber (SBR), acrylonitrile butadiene rubber (ABR), and *cis*-polybutadiene (BR). Their formulations are given in Table I. Similar curves were obtained by Mullins for NR and SBR gum rubbers of different crosslink densities.² The linear part of the curves passing through the origin when extrapolated is in agreement with a theoretical conclusion of Taylor and Darin,¹ based on the finite extensibility of a rubber, that

$$\lambda_{Bs} = \lambda_{Bd} V_r^{1/3} \quad (3)$$

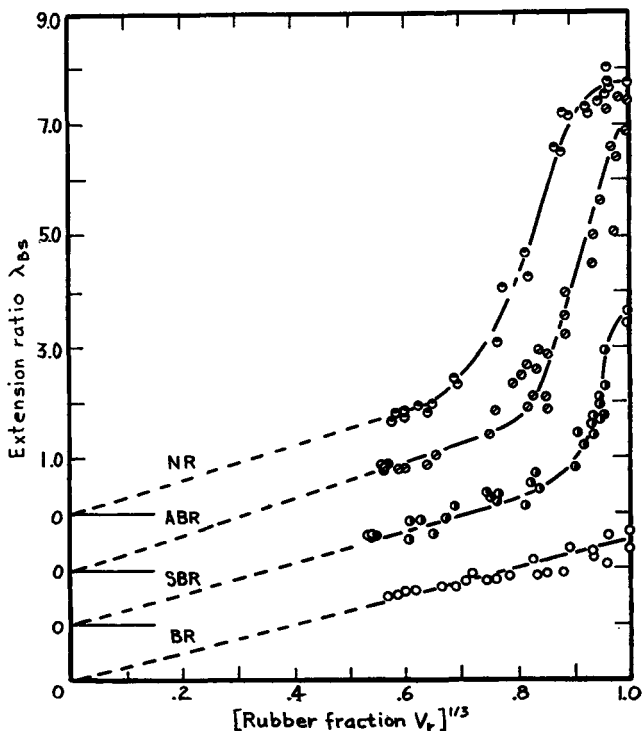


Fig. 1. Extension ratio to break λ_{Bs} , referred to the swollen cross-section, as a function of rubber fraction $V_r^{1/3}$ (the curves have been displaced along the ordinate for clarity): (●) NR; (⊙) ABR; (⊙) SBR; (○) BR.

TABLE I
 Compounding Details*

NR, RSS1	100			
SBR, Intol 1500		100		
ABR, Krynac 801			100	
BR, Cis 1,4				100
Steric acid	2.5	2.5	0.5	2.5
ZnO	3.5	3.5	3.0	3.5
Nonox HFN	1	1	1	1
Santocure CBS	0.6	1.1	—	0.6
MBTS			1.5	
Sulfur	2.5	2.0	1.5	2.0

* Recipes for the black-filled compounds were the same except for the addition of an appropriate amount of processing oil (Dutrex R) with the black filler.

where λ_{Bd} (slope of the linear part) is in this case the hypothetical breaking extension of the dry rubber and is proportional to the number of chain elements between crosslinks. The slopes of all the rubbers examined are very nearly the same, reflecting the fact that all rubbers were cured to approximately the same state of cure.

At high values of V_r (low swelling ratios) the curves rise more sharply with increasing rubber fraction than is predicted by eq. (3), also in agreement with Greensmith et al.,² who attribute this to the action of cohesive forces.

Energy Density at Break. Figure 2 shows the energy density at break for the four gum rubbers as a function of the rubber fraction V_r . The energy density to break has been calculated on unit volume of dry rubber eliminating the dilatational effect and is referred to as U_{Bd} . For BR this appears to be proportional to V_r over the whole experimental range of V_r . A regression analysis of $\log U_{Bd}$ versus $\log V_r$ shows that the best relation to fit the data on the basis of least squares is given by

$$U_{Bd} = 8.85 V_r^{0.79} (\text{kg./cm.}^2) \quad (4)$$

As in the case of the elongation at break, the curves for the other two noncrystallizing rubbers examined, styrene butadiene (SBR) and acrylonitrile-butadiene (ABR), are similar in shape and show a rise at high rubber fractions, which is larger, the smaller the interval between the experimental temperature (21°C.) and the glass transition temperature T_g of the rubber. Moreover, the value of V_r at which the rise becomes obvious decreases with increasing glass transition temperature. Replotting $\log U_{Bd}$ as a function of $\log \xi_g V_r$ produces a single master curve for all three noncrystallizing gum rubbers, as shown in Figure 3. The horizontal shift factors $\log \xi_g$, required to match the ABR and SBR curves to the BR one, are a simple function of the interval T to T_g , as seen from Figure 4. This behavior is similar to that of the complex shear modulus of polymer solutions, described by Ferry.¹⁷ He produced master curves for $G'(t)/C$ and $G''(t)/C$ versus $\log t\eta T_0/\eta_0 TC$, where C is the concentration of the solution, which, of course, is

closely analogous to the rubber fraction V_r in a solvent-swollen rubber. The temperature ratio T/T_0 was constant in all our experiments, and the time t varied only within the narrow limits in which the elongation at break varied, since the experiments were carried out at a constant rate. The

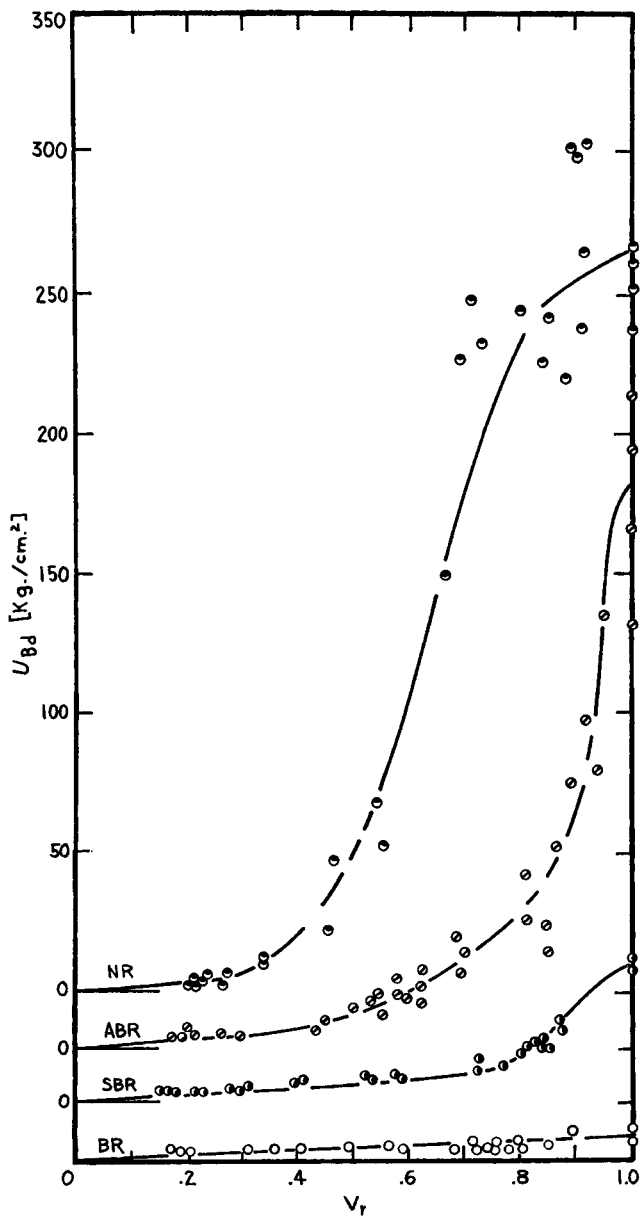


Fig. 2. Energy density to break, U_{Bd} , referred to unit volume of dry rubber, as a function of rubber fraction V_r (the curves have been displaced for clarity); symbols as in Fig. 1.

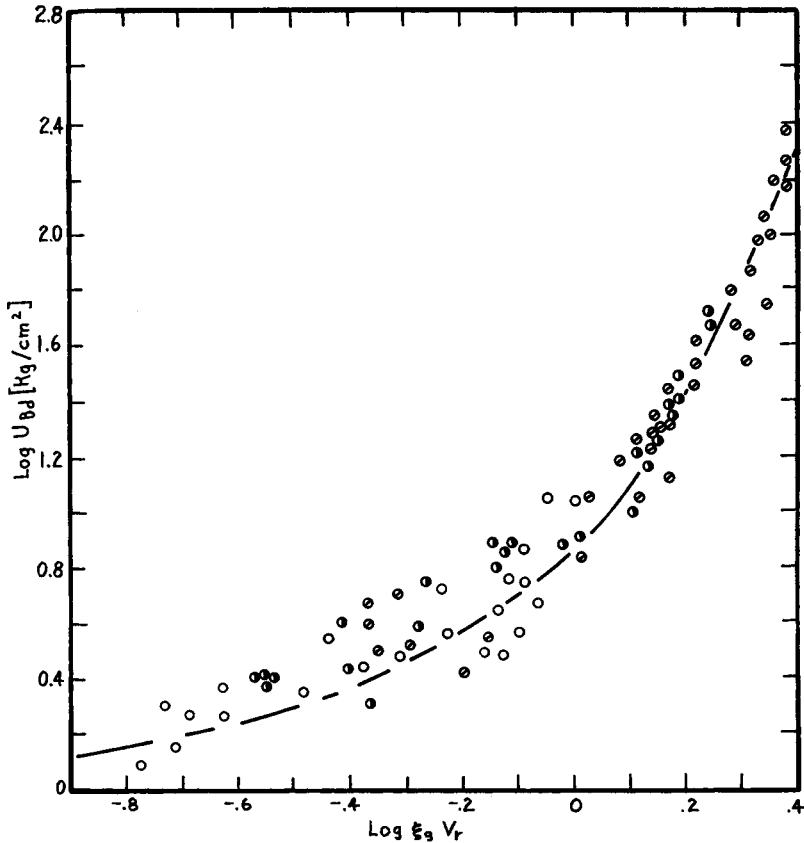


Fig. 3. Energy density to break, U_{Bd} , as a function of the reduced rubber fraction $\xi_0 V_r$; ξ_0 depends on the difference between working and glass transition temperature, as shown in Fig. 4. Symbols as in Fig. 1.

primary contribution to the shift factor $\log \xi_0$ stemmed, therefore, from the relative internal viscosity η/η_0 of the swollen rubber, and this is seen to be proportional to the temperature difference $T - T_g$ at any rubber fraction V_r . Recently Chasset and Thirion showed that the stress relaxation of rubbers at different degrees of swelling could also be reduced to a single factor of log reduced time at constant temperature.¹⁸ The fact that all three rubbers can be superposed to a single master curve indicates that, provided account is taken of differences in the glass transition temperature, the energy density to break is similar for all three rubbers. Previously Mullins⁸ constructed a single master curve of the tearing energy as a function of the reduced rate of tearing for a number of different ABR and SBR rubbers.

The behavior of natural rubber shows departures from this master curve. The $U_{Bd}(V_r)$ has a shape similar to those of the noncrystallizing gum rubbers, but the drop in U_{Bd} occurs at a much lower value of V_r and is more

pronounced. It is well known that natural rubber crystallizes at high strains and that it then becomes very hysteretical under these conditions. The sharp drop in U_{Bd} with decreasing rubber fraction appears, therefore, to be associated with the disappearance of strain crystallization and its accompanying hysteresis.

Breaking Stress. The breaking stress, measured on the swollen sample, has also been referred to unit volume of dry *rubber* and is calculated from the breaking force f_s on the swollen sample as

$$\sigma_{BC} = f_s/a_s V_r k = f_s/a_0 V_r^{1/2} k \quad (5)$$

where k is the volume fraction of rubber in the dry compound ($k = 1.0$ for gum rubbers), and a_0 and a_s are the cross-sectional areas of the dry and swollen samples, respectively. Figure 5 shows $\log \sigma_{BC}$ for the three non-crystallizing gum rubbers plotted as a function of $\log \xi_0 V_r$, with the use of

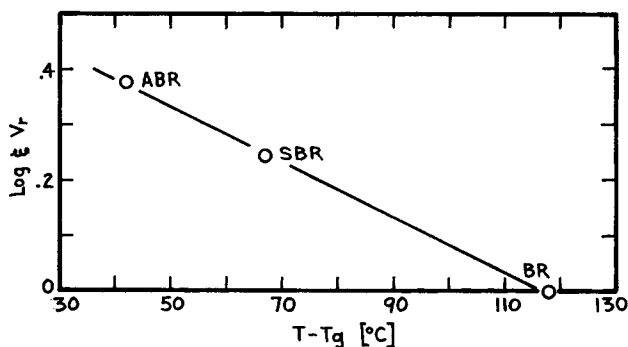


Fig. 4. Horizontal shift factor ξ_0 as a function of difference between working and glass transition temperatures.

the shift factors ξ_0 from Figure 4. It is seen that the three curves assemble to a continuous master curve, which shows a drop in breaking stress with decreasing V_r at high rubber fractions. At lower rubber fractions the changes in breaking stress per unit volume of rubber become smaller than the experimental scatter, and σ_{BC} appears to become independent of $\xi_0 V_r$. Examination of the stress-strain curves in this region shows that the stress does not change much with increasing strain, at the breaking strains which are in the region of 75–100%. In the present plot on a logarithmic scale this region appears very much extended. Similar behavior was observed by Smith for the rate dependence of the breaking stress of an SBR gum rubber.⁵ Changes in energy density to break in this region of high swelling ratios therefore stem essentially from changes in extensibility. Because the hysteresis in the bulk of the rubber is very small, and the rubber breaks at such low strains, the stress-strain curve can be described right up to break by the C_1 term in the Mooney-Rivlin¹⁹ equation:

$$f_s = 2C_1 V_r^{1/3} (\lambda - 1/\lambda^2) \quad (6)$$

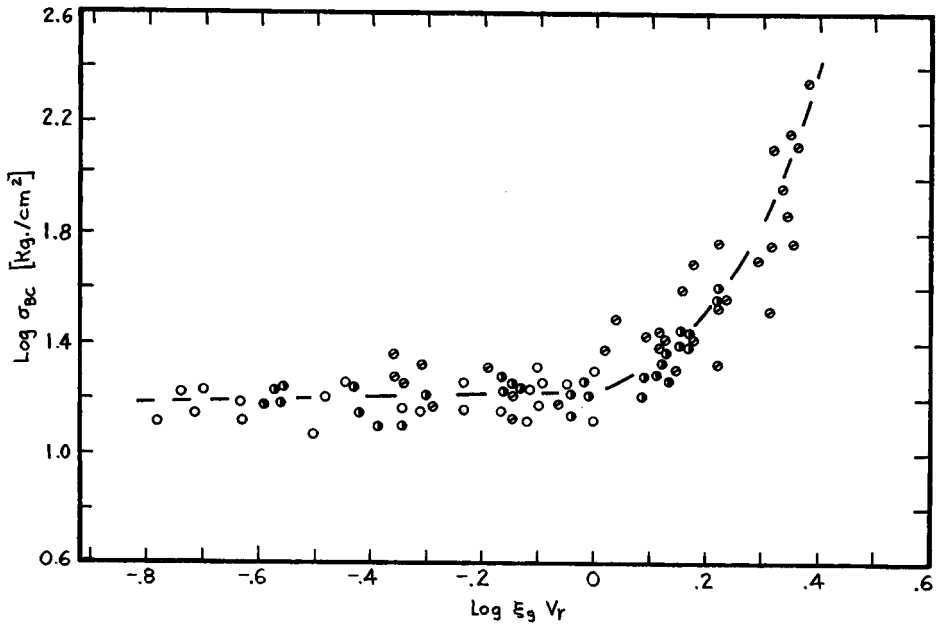


Fig. 5. Breaking stress σ_{BC} per unit concentration of rubber, as a function of reduced rubber fraction $\xi_0 V_r$, for the three noncrystallizing gum rubbers. Symbols as in Fig. 1.

If the breaking stress is derived by inserting the breaking extension ratio in this equation, then the breaking stress is proportional to the stiffness of the rubber, which is given by

$$2C_1 = NkT/M_c$$

The breaking stresses of different gum rubbers could thus only be assembled as a master curve by horizontal shift, because the rubbers were compounded and cured to the same crosslink density and had similar C_1 values. If rubbers of different crosslink density had been used, account would have had to be taken of differences in the equilibrium modulus C_1 .

Natural rubber, again, shows departures from this behavior; the high tensile strength resulting from crystallization persists to quite low values of V_r (see Fig. 9, bottom curve). At even lower values of V_r , crystallization is absent, and the breaking stress is similar to that of noncrystallizing rubbers at the same state of swelling. A similar phenomenon has been observed for the temperature dependence of tensile strength.^{9,10}

Effect of Black Fillers

Breaking Stress. Figure 6 shows the breaking stress σ_{BC} as a function of the rubber fraction V_r for SBR, filled with different amounts of HAF black. The curves are similar in shape to those of gum rubbers, discussed previously. They show a decrease in breaking stress with decreasing V_r ,

and the magnitude of the decrease of stress increases with increasing black concentration. Below a certain value of V_r , which decreases with black concentration, the breaking stress σ_{BC} shows less variation with V_r than the experimental scatter and appears, as in the case of gum rubbers, to tend

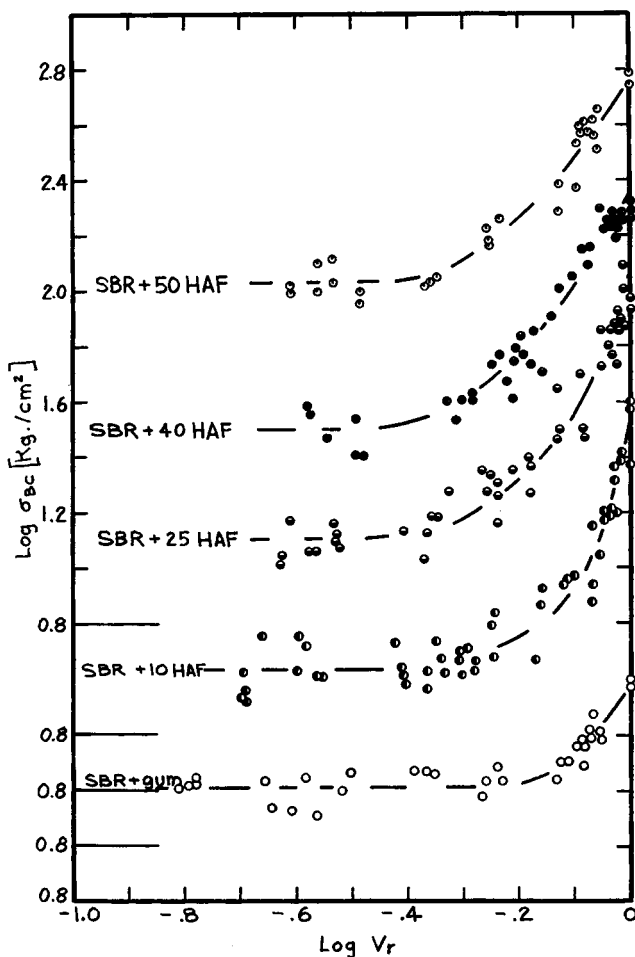


Fig. 6. Breaking stress σ_{BC} of SBR, filled with different concentrations of HAF black, as a function of the rubber fraction V_r . (the curves have been displaced along the ordinate for clarity).

toward a limiting value. This limiting value, however, increases with black concentrations; see Table II. Table II also gives the limiting breaking stresses for NR and BR compounds filled with different concentrations of HAF black, and for SBR and BR filled with different types of black at a constant concentration of 50 pphr.

TABLE II
Breaking Stresses $\sigma_{BC}/(\text{kg./cm.}^2)$ for Highly Swollen Rubbers

	NR	SBR	BR
Gum	24.0	16.2	16.2
+ 10 HAF	39.8	26.6	25.1
+ 25 HAF	66.1	59.3	46.8
+ 40 HAF	91.2	78.5	135
+ 50 HAF	100	105	126
50 MT	—	52.5	52.5
50 ISAF	—	109	145

As in the case of the gum rubbers, the limiting values of the breaking stress are influenced by the equilibrium modulus E . This increases with the black concentration according to a relation of the type²⁰

$$E = E_0(1 + 0.67fC + 1.62f^2C^2) \quad (7)$$

where E_0 is the modulus of the unfilled compound, C is the volume concentration of black filler, and f is a shape factor, allowing for the fact that the filler particles agglomerate into rod-like assemblies. By using shape factors of 6 to 7 the breaking stresses at high swelling ratios of all the black-filled compounds can be explained in terms of increased stiffness. Since eq. (7) is based on the assumption that the carbon black adheres to the rubber, the fact that the increase in tensile strength in the highly swollen state with filler concentration can be explained by this equation must mean that energy absorption by incipient failures between rubber and black is probably not a very significant source of hysteresis contributing to the reinforcement of carbon-black-filled rubbers, as has been suggested in the literature.²¹

The breaking-stress curves for a particular rubber and type of black but for different concentrations can be reduced to a single master curve, in this case by vertical as well as horizontal shifts on a doubly logarithmic plot, as shown in Figure 7 for SBR filled with HAF, MT, and ISAF (lower, middle,

TABLE III
Vertical Shift Factor $\log p$ as a Function of
Concentration and Type of Filler

	From data on breaking stress		From data on energy density at break	
	SBR	BR	SBR	BR
Gum	0	0	0	0
+ 10 HAF	0.21	0.21	0.05	0.20
+ 25 HAF	0.51	0.43	0.09	0.20
+ 40 HAF	0.70	0.90	0.13	0.55
+ 50 HAF	0.81	0.90	0.15	0.59
+ 50 MT	0.50	0.50	0.20	0.50
+ 50 ISAF	0.80	0.95	0.20	0.95

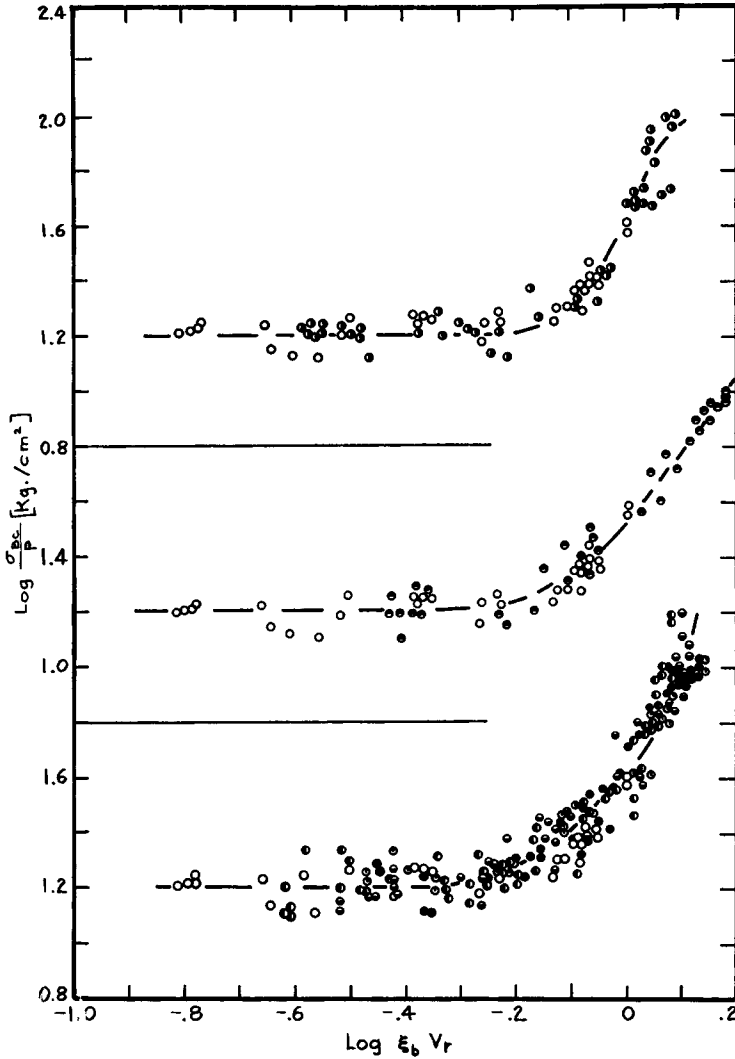


Fig. 7. Reduced breaking stress σ_{BC}/p of SBR, filled with different concentrations of (lower graph) HAF black, (middle) ISAF, and (upper graph) MT, as a function of reduced rubber fraction $\xi_b V_r$: (O) gum; (●) 10 HAF; (⊖) 25 HAF; (⊗) 40 HAF; (⊙) 50 HAF; (⊕) 50 ISAF; (⊙) 50 MT.

and upper curves, respectively); similar curves are shown in Figure 8 for BR filled with the same types of black.

The vertical shift factors p , shown in Table III as $\log p$, are the factors by which the breaking stress of a black-filled rubber at low values of V_r must be divided to make it coincide with the value of the corresponding gum rubber and are identical with the ratios of their respective moduli, as discussed above. Recently, Harwood and Payne showed that this stiffening is also accompanied by a corresponding increase in hysteresis,²² the

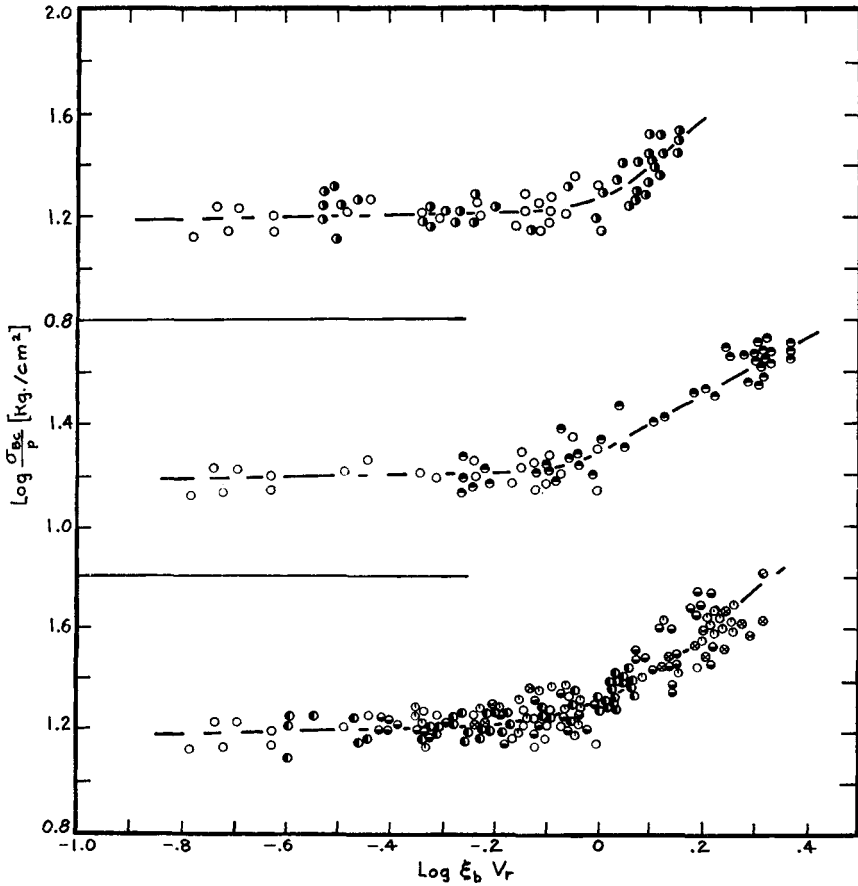


Fig. 8. Reduced breaking stress $\sigma_{BC/P}$ of BR, filled with different concentrations and types of black, as a function of reduced rubber fraction $\xi_b V_r$. Symbols as in Fig. 7.

hysteresis in a black-filled rubber being larger than that in the gum rubber by a factor equal to the ratio of the moduli according to eq. (7).

The horizontal shift factors ξ_b , shown in Table IV increase with the black concentration. For the gum rubbers the shift factors ξ_g were a simple function of the temperature difference between the experimental and the glass transition temperatures and were associated with the internal friction of the rubber network. In this case, too, the horizontal shifts $\log \xi_b$ are due to hysteresis in the rubber network, which in this case is increased by the carbon black. This view is supported by the increase in glass transition temperature observed with increasing black filler concentration.^{23,24} However, this observed increase is less than would be expected from a comparison of ξ_b and ξ_g values. Figure 4 shows that a shift factor $\log \xi_g$ of 0.14 is equivalent to a difference in glass transition temperature of approximately 26°C. between two different gum rubbers. A similar shift of $\log \xi_b$ caused by an increase in the black concentration from 0 to 50 HAF in SBR,

TABLE IV
Horizontal Shift Factor $\log \xi_0$ as a Function of Concentration and Filler Type

	From data on breaking stress		From data on energy density at break	
	SBR	BR	SBR	BR
Gum	0	0	0	0
+ 10 HAF	0.08	0.065	0.08	0.10
+ 25 HAF	0.105	0.21	0.105	0.14
+ 40 HAF	0.13	0.25	0.125	0.25
+ 50 HAF	0.14	0.31	0.13	0.31
+ 50 MT	0.08	0.15	0.08	0.15
+ 50 ISAF	0.175	0.37	0.18	0.37

however, produces only a difference in glass transition temperature of about 7°C. It is therefore plausible that the increase in internal friction is not uniform throughout the network but is more pronounced in the vicinity of the carbon black particles, most likely in the form of a locally higher concentration of network chains. Such "shells" of rubber around the black particles have been shown by Westlinning et al.²⁵ to exist in natural rubber where the cohesive forces are large enough for the natural rubber to show crystallization at room temperature in the unstrained condition.

Both vertical and horizontal shift factors depend on the types of black and rubber. The finer the black particles, the larger the shift factors. They are probably also influenced by the black dispersion. In the case of vertical shift factors this can be explained by differences in the shape factor f in eq. (7); i.e., different types of black form rod-like assemblies of different length-to-width ratio. The phenomenon could, however, equally well be explained by the existence of thin shells of rubber around the black particles, as discussed above. The latter also may contribute to differences between the horizontal shift factors that are observed for different types of black, finer blacks of greater surface activity absorbing a thicker layer of rubber and, hence, restricting the network more than coarser blacks.

The horizontal shift factors also depend pronouncedly on the type of rubber; they are much larger for BR than for SBR. It appears that the more hysteresis at high strains, the smaller the horizontal shifts. Clearly, the hysteresis in a compound in which the chains are already hindered in their motion is less affected by a further constriction in the vicinity of carbon filler particles than is the case of a highly mobile network.

For NR vulcanizates containing different concentrations of HAF black or different types of black the breaking stress shows a sharp drop always at the same value of V_r , as is apparent from Figure 9. Hysteresis and, hence, strength is derived predominantly from crystallization, and the results show that this disappears always at the same value of V_r , regardless of the black filler concentration and type. The effect of stiffening on the strength, however, is apparent from the increase in breaking stress with black concentration at low V_r .

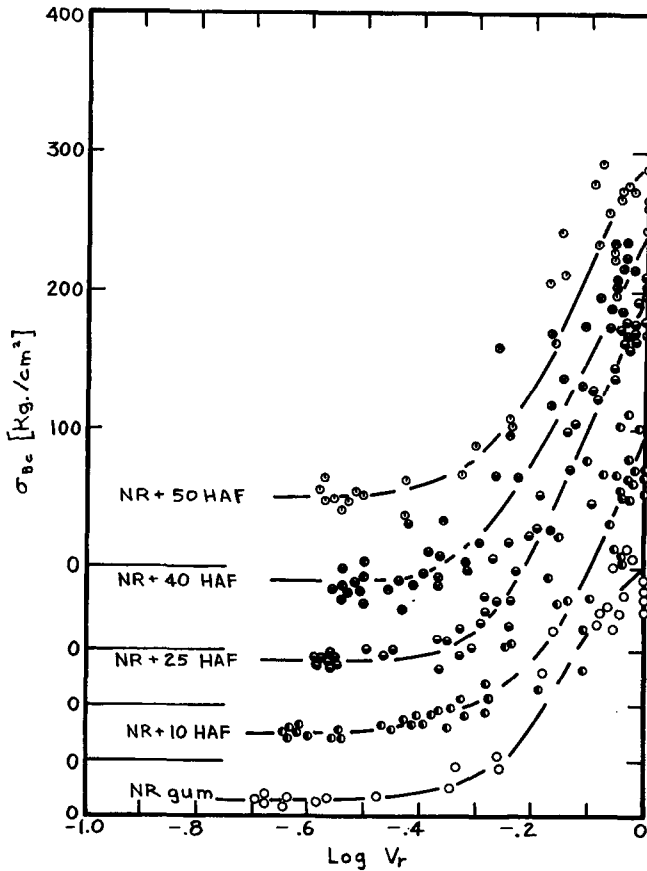


Fig. 9. Breaking stress σ_{BC} of NR, filled with different concentrations of HAF, as a function of rubber fraction V_r (the curves have been displaced along the ordinate for clarity). Symbols as in Fig. 7.

In all other regions crystallization dominates the strength behavior, and no transformation of the results is possible.

Energy Density to Break. Figure 10 shows the energy density at break, U_{Ba} , referred to unit volume of rubber for SBR, filled with different concentrations of HAF black, as a function of V_r . As in the case of the breaking stress curves, all curves are similar in shape. The curves can also be reduced to a single master curve of $\log U_{Ba}/p$ versus $\log \xi_b V_r$. It is found that for SBR (Fig. 11) and BR (Fig. 12) the best fit is obtained by using ξ factors that agree closely with those found for the reduction of the stress curves (see Table IV). The p factors for BR are also similar to those derived from stress data. For SBR, however, they are much smaller, as can be seen from Table III. Examination of the stress-strain curves to break showed that the extension at break is also affected by the addition of black.

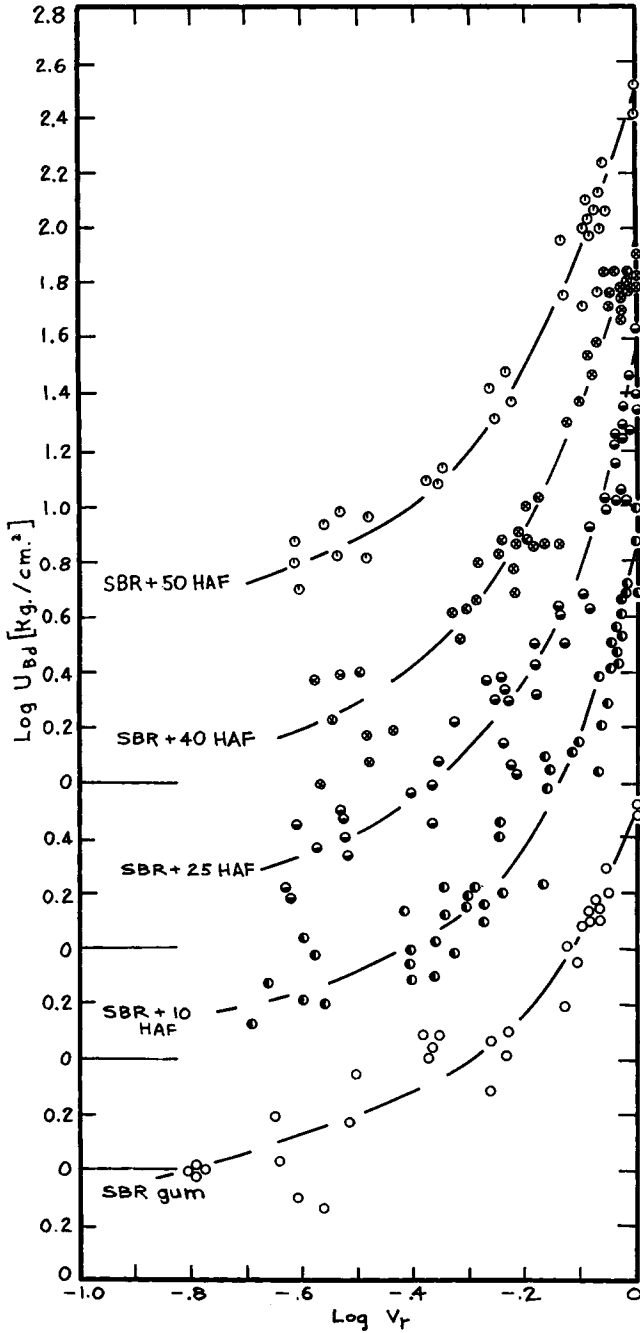


Fig. 10. Energy density at break U_{Bd} for SBR, filled with different concentrations of HAF black (the curves have been displaced for clarity). Symbols as in Fig. 7.

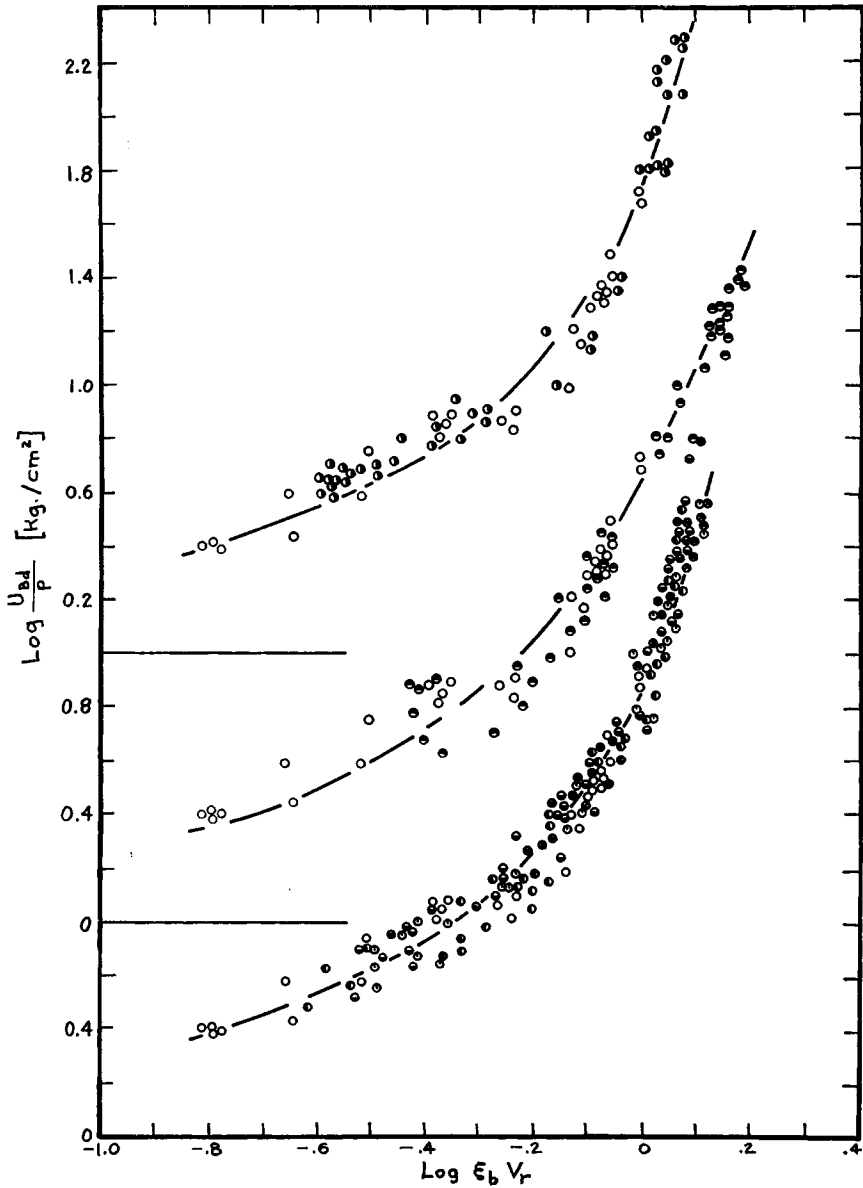


Fig. 11. Reduced energy density at break, $U_{Bd/p}$ for SBR, filled with different types of black, as a function of reduced rubber fraction $\epsilon_b V_r$. Symbols as in Fig. 7.

For SBR it is somewhat reduced by increasing the black concentration, whereas for BR the extensibility increases with black concentration. This means that the gain in energy needed to break the rubber by filler incorporation is much larger in BR than in SBR for the same black filler content. Presumably, the proportionality between bulk properties and the proper-

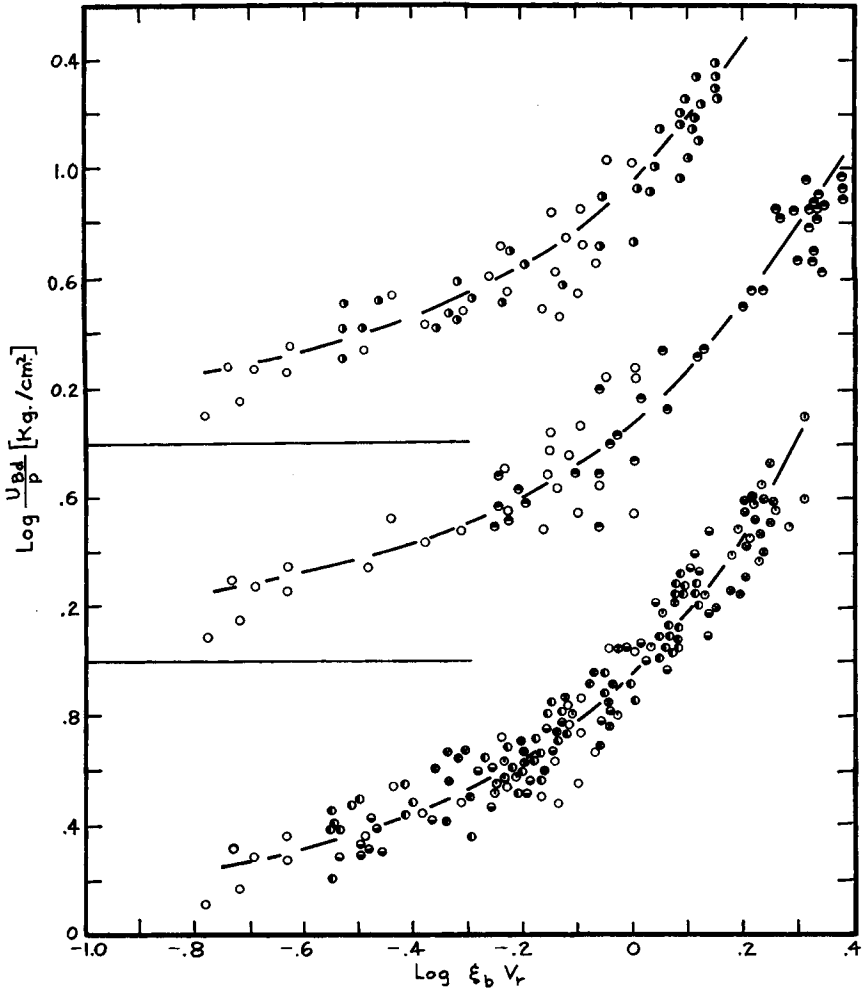


Fig. 12. Reduced energy density at break, $U_{Bd/p}$ for BR, filled with different types of black, as a function of reduced rubber fraction $\xi_b V_r$. Symbols as in Fig. 7.

ties at the tip of the advancing tear, which is a basic assumption in all this work, is no longer fulfilled. It is known that BR can crystallize at certain temperatures and at large strains, and hence it is possible that strain crystallization occurs at the tip of the tear of black-filled BR, where both strain amplification due to black filler and the stress concentrations at the tip of the tear combine to produce very large strains, whereas in the bulk of the rubber the strains are not large enough to produce any significant crystallization. That this can happen only to a limited extent is obvious from the general behavior of BR, which was in our experiments much more like that of a noncrystallizing rubber. However, small anomalies in the strength behavior of BR, not unlike the very pronounced anomalies in the

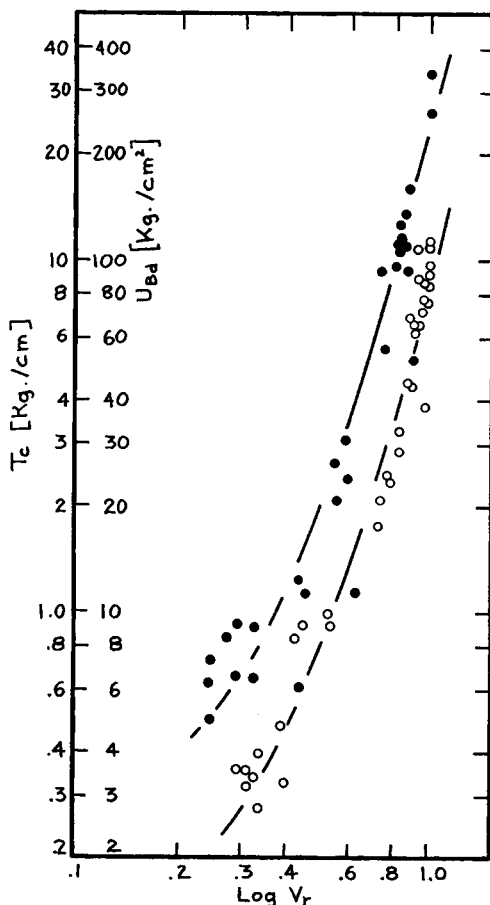


Fig. 13. Tearing energy T_c (O) and energy density at break U_{Bd} (●) for SBR + 50 HAF, as a function of rubber fraction V_r .

behavior of NR, were observed by Harwood and Payne,²⁶ who therefore came to a similar conclusion.

The master curves of $\log U_B/p$ versus $\log \xi_b V_r$ are all of similar shape and can be described by a single relation:

$$U_{Bd}/p = U_{B0} \exp \{ \alpha' V_r \} \quad (8)$$

Moreover, if the factor α' is written as

$$\alpha' = \alpha \xi_b / \xi_g \quad (8a)$$

where ξ_b and ξ_g are the horizontal shift factors for the carbon black filler concentrations and the difference in glass transition temperature between two gum rubbers, respectively, all the curves can be referred to a single reference curve, which in this case was chosen as that for gum BR, because it had the lowest glass transition temperature. The two coefficients U_{B0}

TABLE V
Coefficients^a

	U_{B_0}	α
Different gum rubbers	1.20	0.89
BR diff. HAF		
concs.	1.29	0.91
SBR diff. HAF concs.	1.30	0.91
BR diff. ISAF concs.	1.48	0.74
SBR diff. ISAF concs.	1.27	0.91
BR diff. MT concs.	1.35	0.85
SBR different MT concs.	1.51	0.88

^a Coefficients in $U_{B_0}/p = U_{B_0} \exp \{ \alpha (\xi_b/\xi_g) V_r \}$, where ξ_b = reduction factor for rubber fraction in black-filled rubbers, and ξ_g = reduction factor for rubber fraction in gum rubbers of different $T - T_g$.

and α are then constants, independent of type of rubber and type and concentration of black filler, as shown in Table V.

Equation (8) resembles in form a relation due to Arrhenius,²⁷ describing the concentration dependence of the viscosity of solutions:

$$\eta/\eta_0 = A \exp \{ \alpha C \} \quad (9)$$

This close similarity between the strength behavior of a swollen rubber and the viscosity of a solution demonstrates again the important role that viscous processes play in the strength behavior of rubbers.

Tearing Energy

Figure 13 shows the tearing energy²⁸ T obtained from trouser test pieces for SBR + 50 HAF black. Also shown is the energy density to break, and it is seen that the tearing energy is proportional to the energy density at break over the whole range of swelling ratios. Such a result is to be expected, if it is recognized that tensile failure is really a catastrophic tearing phenomenon starting from inherent flaws in the material.²⁹ For the type of test piece used in this investigation the critical tearing energy T_C at which the test piece will fail catastrophically is related to the energy density at break by^{28,30}

$$T_C = 2KC_0U_B \quad (10)$$

where C_0 is the initial flaw size from which rupture starts, and k is a factor. The flaw size is expected to increase with the cube root of the swelling ratio and is therefore not greatly influenced by swelling; k decreases somewhat with increasing strain, assisting to compensate the increase in C_0 , so that the variation of $2KC_0$ does not exceed 25% over the whole range of swelling ratios. From Figure 13 it appears that $2kC_0 \approx 4 \times 10^{-2}$ and that, with $k = 4$, $C_0 \approx 5 \times 10^{-3}$ cm., a value for the flaw size which is in close agreement with other estimates.³¹

Hysteresis at High Strains

All the arguments above indicate that the energy density at break of dry to highly swollen rubbers is dominated by the hysteresis that obtains in the rubber at high strains. To verify this quantitatively, experiments were carried out to determine the hysteresis of a number of rubbers, both dry and swollen, near the breaking condition by extending a test ring and reversing the extension direction near the previously determined breaking extension. New test rings were used in each case, and temperature and extension rate were kept at the same value as in all experiments described

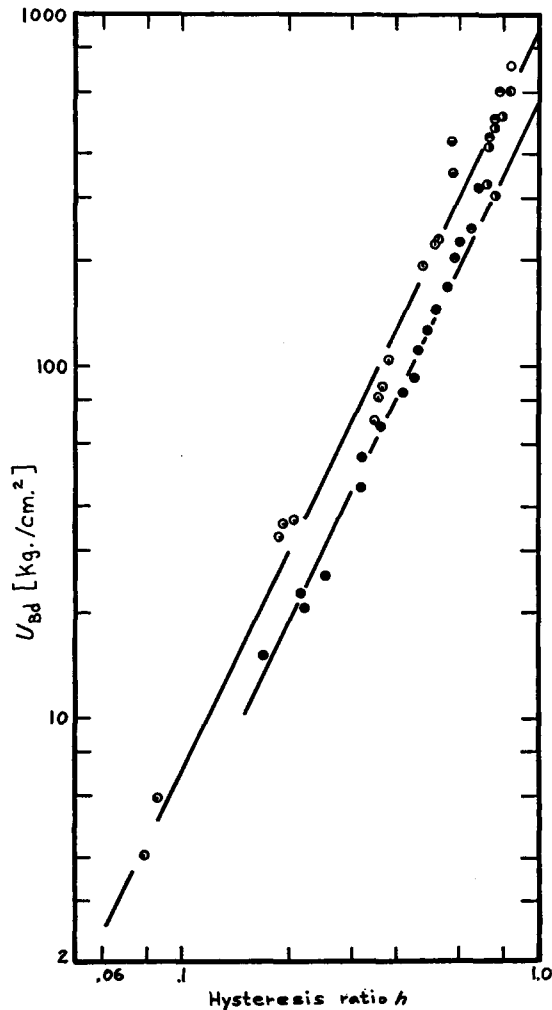


Fig. 14. Energy density at break, U_{Bd} , as a function of hysteresis ratio h , measured near breaking condition: (⊗) SBR + 50 HAF, different swelling ratios; (⊙) gum BR; (⊖) gum SBR; (⊕) gum ABR; (⊙) gum NR; (⊗) NR + 50 HAF; (⊖) ABR + 50 HAF; (⊙) SBR + 50 HAF; (⊖) BR + 50 HAF.

previously. In Figure 14 the energy density input, which was statistically not different from the energy density at break, is plotted as a function of the hysteresis ratio h_b near break, where h_b is the energy lost divided by the energy input in the first stress-strain cycle taken to near-breaking condition. The two lines drawn through the experimental points are both given by the following equation:

$$U_{Bd} = qh^n \quad (11)$$

The index n is in both cases 2.10, and a more detailed investigation, with temperature as variable and a wide range of rubbers, has shown that this is always the case.³²

The factor q is 880 kg./cm.² for the dry rubbers, irrespective of type of rubber and whether it contains a black filler or not. The more detailed investigation, referred to above, has shown that different rubbers can give small but significantly different factors,³² and this value must be considered an average one. The lower factor for the SBR + 50 HAF, swollen to different rubber fractions, therefore probably is not due to an effect of swelling but is associated with the rubber.

The hysteresis was in all cases measured on new rings and included, therefore, hysteresis due to stress softening (Mullins effect).¹¹ Although confined to the first few stress-strain cycles, this energy has to be expended before the rubber can be brought to the breaking condition, and may constitute a major fraction of the total measurable hysteresis.

CONCLUSION

The swelling of a rubber in a low-viscosity liquid decreases in general the breaking stress, the energy density at break, and the elongation at break, of that rubber. The magnitude of the change may be quite small or very large, depending on a number of factors. In the case of noncrystallizing gum rubbers the changes are the larger, the smaller the interval between working temperature and glass transition temperature. For black-filled rubbers the change increases with black concentration and differs for different types of filler at the same concentration. It is larger for fine-particle fillers of high surface activity than for coarse fillers. For strain-crystallizing natural rubber the effect of swelling is always large, once a critical swelling ratio, which itself is large, has been exceeded.

In all cases the general shapes of the strength (V_r) curves are similar, and for noncrystallizing gum rubbers the breaking stress and energy density to break can be assembled into a single master curve by multiplying the rubber fraction V_r by a factor ξ_r which depends only on the difference between working and glass transition temperature. Similarly, curves of breaking stress and energy density to break for a noncrystallizing rubber filled with different concentrations of a particular type of black can be assembled into a master curve by multiplying the strength parameter by a factor $1/p$ and the rubber fraction V_r by a factor ξ_b , where both p and ξ_b are functions of the

black concentration. The factor p is shown to be related to the stiffening effect which the black filler has on the compound; the factor ξ_b , on the other hand, is probably a function of the intrinsic viscosity of the polymer, as is strongly suggested by the close analogy with the behavior of the non-crystallizing gum rubbers with different glass transition temperatures. Finally, the shape of the master curves of the energy density to break can be described by an exponential function of the reduced rubber fraction ξV_r , a relation which is similar in form to that of the concentration dependence of the viscosity of polymer solutions.

All the evidence suggests that the strength behavior of a swollen rubber is dominated by the hysteresis which obtains in the rubber near break, and this is substantiated by the demonstration that energy density at break and hysteresis at break are linked by a single empirical relation which, apart from a factor, is independent of type of rubber and filler.

The investigation also throws some further light on the reinforcement mechanism of carbon fillers. The increased hysteresis in black-filled rubbers, responsible for the increased strength, is seen to have at least two origins. First, the well-known stiffening action of the black also contributes to the strength. For rubbers of the same degree of crosslink density the breaking stress is the bulk stress necessary to propagate a crack through the test piece, at equal breaking extension, and will be roughly in proportion to the stiffnesses. Second, even after allowing for the stiffening effect, the breaking stress and energy density at break are higher for a black-filled rubber than for the corresponding gum rubber, at high rubber fractions. In this region a larger swelling ratio, or smaller rubber fraction, is required to reduce the strength of a black-filled rubber to that of the gum rubber. This behavior indicates that the black filler increases the hysteresis in the rubber phase, probably preferentially in the vicinity of the rubber-black interface, as the relatively small shifts in the glass transition temperature indicate.

This work forms part of a Research program undertaken by the Natural Rubber Producers' Research Association. The author wishes to thank Miss B. Arundell and Mr. P. Levene for assistance with the experimental work.

References

1. G. R. Taylor and S. R. Darin, *J. Polymer Sci.*, **17**, 511 (1955).
2. H. W. Greensmith, L. Mullins, and A. G. Thomas, in *The Chemistry and Physics of Rubber-Like Substances*, L. Bateman, Ed., MacLaren, London, 1963, p. 262.
3. A. J. Wildschut, *Technological and Physical Investigations on Natural and Synthetic Rubbers*, Elsevier, Amsterdam, 1946, p. 149.
4. B. A. Dogadkin, D. L. Fedycikin, and V. E. Gul, *Rubber Chem. Technol.*, **31**, 756 (1958).
5. T. L. Smith, *J. Polymer Sci.*, **32**, 99 (1958).
6. L. Mullins, *Trans. Inst. Rubber Ind.*, **35**, 213 (1957).
7. G. Gee, *J. Polymer Sci.*, **2**, 451 (1947).
8. L. Mullins, *Trans. Inst. Rubber Ind.*, **32**, 236 (1956).
9. B. S. T. T. Boonstra, *India Rubber World*, **121**, 300 (1949).

10. A. G. Thomas, in *Use of Rubber in Engineering*, P. W. Allen et al., Eds., McLaren, London, 1967.
11. L. Mullins, *Trans. Inst. Rubber Ind.*, **33**, 5 (1956).
12. E. M. Dannenberg, *Trans. Inst. Rubber Ind.*, **42**, T26 (1966).
13. G. Kraus, C. W. Childers, and K. W. J. Rollman, *J. Appl. Polymer Sci.*, **10**, 229 (1966).
14. R. Peremsky, *Kauchuk a plastice hmoty*, **2**, 429 (1962), *Rubber Plastics Res. Assoc.*, 1247.
15. K. A. Grosch and L. Mullins, *Rev. Gen. Caoutchouc*, **39**, 1781 (1962).
16. J. A. C. Harwood, A. R. Payne, and L. Mullins, *Inst. Rubber Ind. J.*, **1**, 17 (1967).
17. J. D. Ferry, *J. Am. Chem. Soc.*, **72**, 3748 (1955).
18. R. Chasset and P. Thirion, *Proc. Intern. Conf. Phys. Noncrystalline Solids*, J. A. Prins, Ed., North-Holland, Delft, 1964, p. 346.
19. L. R. G. Treloar, *Physics of Rubber-Like Elasticity*, Oxford Univ., Press, 1949.
20. E. Guth, *Proc. 2nd Rubber Technol. Conf. (London)*, 1948, p. 353; *J. Appl. Phys.*, **16**, 20 (1945).
21. E. H. Andrews and A. Walsh, *Proc. Phys. Soc.*, **42**, 72 (1958).
22. J. A. C. Harwood and A. R. Payne, private communication.
23. A. R. Payne, *Rheology of Elastomers*, P. Mason and M. Wookey, Eds., Pergamon, New York, 1958, p. 86.
24. R. F. Landel and T. L. Smith, *ARS (Am. Rocket Soc.) J.*, 599 (1961).
25. H. Westlinning, G. Butenuth, and G. Leine-Weber, *Makromol. Chem.*, **50**, 253 (1961).
26. J. A. C. Harwood and A. R. Payne, *J. Appl. Polymer Sci.*, **12**, 889 (1968).
27. S. Arrhenius, *Medd. Vetenskapakad Nobel Trust*, **4**, 13 (1916).
28. R. S. Rivlin and A. G. Thomas, *J. Polymer Sci.*, **10**, 291 (1953).
29. F. Bueche, *Rubber Chem. Technol.*, **32**, 1269 (1959).
30. H. W. Greensmith, *J. Appl. Polymer Sci.*, **8**, 1113 (1964).
31. G. J. Lake and P. B. Lindley, *J. Appl. Polymer Sci.*, **9**, 1233 (1965).
32. K. A. Grosch, J. A. C. Harwood, and A. R. Payne, in *Physical Basis of Yield and Fracture*, Inst. Physics Conf., Oxford, 1966, p. 144.

Received July 21, 1967

Revised August 29, 1967